J Electroceram (2012) 28:123–131
DOI 10.1007/s10832-012-9692-9

Compact size ultrasonic linear motor using a dome shaped piezoelectric actuator

Man-Soon Yoon · Neamul Hayet Khansur · Kyung-Sun Lee · Young Min Park

Received: 17 December 2009 / Accepted: 9 February 2012 / Published online: 29 February 2012
© Springer Science+Business Media, LLC 2012

Abstract This paper presents original results obtained in the development of dome-shaped actuator for a linear motor application. The main structure of compact ultrasonic linear motor presented in this paper consists of three parts, which were an actuating part, a shaft and mobile element. The actuating part was fabricated by powder injection molding (PIM) process. The linear motion of new-type linear motor was operated by the principle of inertia displacement. The actuating part combined with clamping ceramic element can be realized by the central movement of dome-shaped piezoelectric actuator (DSPA), which has the maximum displacement of the up-and-down movement. The linear motor, where DSPA was 9.86 mm in diameter, 4.6 mm in curvature of radius and 0.4 mm in thickness, operated at 1st resonance frequency. The dynamic characteristics of the motor was investigated by finite element method (FEM) and compared with experimental results. These results were in good agreement with that predicted by simulations.

Keywords Powder injection molding · PZT · Actuators · Sensors · Dome shape

M.-S. Yoon (✉) · N. H. Khansur
Department of Materials Sci. and Eng./Research Center for Sustainable Eco-Devices and Materials (ReSEM), Chungju National University, Chungbuk 380-702, South Korea
e-mail: msyoon@cjnu.ac.kr

K.-S. Lee
R&D center, INOVA. Inc., Chungju National University, System Building 203, Chungbuk 380-702, South Korea

Y. M. Park
Research Institute of Industrial Science and Technology, Fuel Cell Project, #32 Hyoja-Dong, Nam-Gu, Pohang City, 790-330, Gyeongbuk, South Korea

1 Introduction

Conventional bimorph bending actuators are composed of two piezoelectric plates, or two piezoelectric plates and an elastic shim, bonded together. The bonding layer causes an increase in hysteresis and a degradation of the displacement characteristics, as well as delamination problem [1]. Furthermore, the fabrication process for such devices, which involves cutting, polishing, electroding and bonding step, is rather laborious and costly. Multilayer structure also can not avoid above problem. The multilayer structure is essentially comprised of alternating ferroelectric and conducting layers, which are co-fired to produce a dense, cohesive unit. The ferroelectric layer sandwiched between a pair of electrodes constitutes a single ferroelectric element. Hundreds of these thick films are connected in parallel and electric filed is supplied by the external electrodes. In this type of structure, generation of internal crack between the layers under bipolar drive caused by alternating strain is a common problem. Therefore, design of reliable device is the key issue.

Thus, there are needs for new type actuator without a layer structure, a bonding process etc. Such a new type monolithic device has been produced from powder injection molding process which is suitable to mass production without any restrictions such as size, materials etc. Piezoelectric and electrostrictive ceramic materials have been widely used as solid-state actuators [2–4]. Despite of their enormous applications, the direct extensional strain in most piezoelectric or electrostrictive ceramic materials is at best a few tenths of one percent. Thus, it is essential to develop the method to amplify the strain of devices.

Compared with a normal electromagnetic motor, which has a high efficiency but a low torque at a low speed, the ultrasonic motor can produce a high torque at a low speed with high efficiency. An ultrasonic motor is an attractive

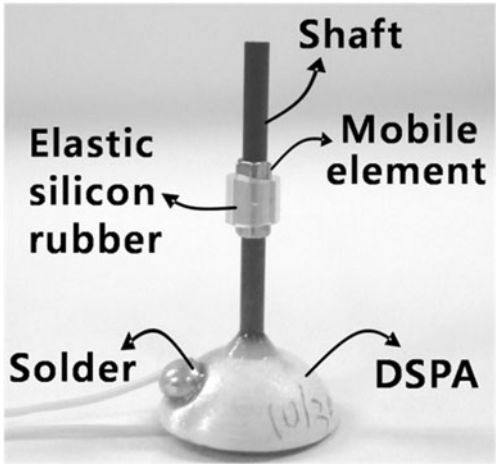

Fig. 1 Photograph of the DSPLM

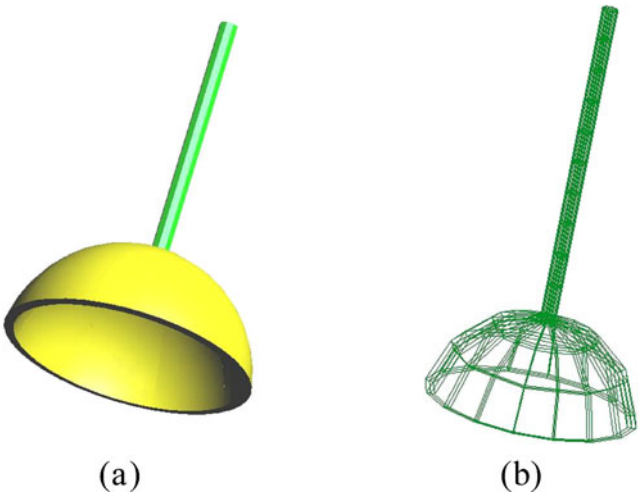

Fig. 3 3-dimensional structure combined with shaft (**a**) and Finite Element mashes used for DSPA analysis (**b**)

device in application for an imaging process such as optical zoom, hand shake protection in digital camera. There are several ways to transform the piezoelectric vibration into the linear sliding movement such as non-self-moving and/or self-moving types [5]. However, the complex structure and circuit of conventional ultrasonic linear motors limit the adaptation to the optic zoom of the mobile communication hand sets and compact digital camera. For example, the piezoelectric inertia linear motor using a multilayer actuator has been developed by Konica Minolta, which is used for the camera-shake correction and the control of zooming, auto-focusing and the aperture of micro-camera that is required to be downsized. [6]

In this work, new type of ultrasonic piezoelectric actuator, which is able to provide higher displacement than classical ultrasonic actuator based on bimorph and multi layer actuator, is proposed. It is composed of dome-shaped piezoelectric ceramic manufactured by **p**owder **i**njection **m**olding (PIM) process and bottom-clamped ceramic element in order to increase the Z-axis displacement.

FEM software has been used as analysis tool. Performances of the proposed ultrasonic piezoelectric actuator have been balanced against the non-clamped **d**ome-**s**haped **p**iezoelectric **a**ctuator (DSPA).

Finally, in order to evaluate the continuous linear motion, newly designed linear motor using the proposed DSPA was produced and the dynamic characteristic was demonstrated with inertia weight.

2 Structure and operation principle

2.1 Structure

Figure 1 is an exemplary construction of a **d**ome-**s**haped **p**iezoelectric **l**inear **m**otor (DSPLM). The motor consists of the three parts, which are actuating component, drive shaft and mobile element. The actuating component contains DSPA fabricated by PIM. The displacement of actuating component is to transfer into the drive shaft. The shaft is located at the center of the DSPA. The mobile element is coupled with the outer shaft combined with an elastomer. The frictional force can be controlled by the elastic force of the silicon rubber.

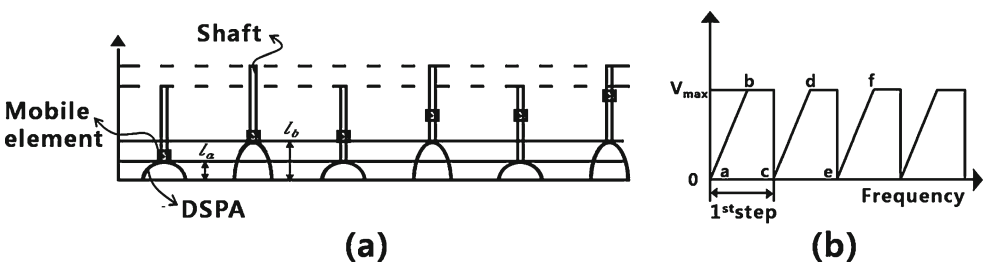

Fig. 2 The principle of inertia displacement (**a**) and (**b**) saw tooth electrical potential

Table 1 PZT5AH data used for this modeling

s_{11}^E [m^2/N]	s_{12}^E [m^2/N]	s_{13}^E [m^2/N]	s_{33}^E [m^2/N]	s_{44}^E [m^2/N]
16.4×10^{-12}	-4.7×10^{-12}	-7.22×10^{-12}	20.8×10^{-12}	47.5×10^{-12}
d_{15} [C/N]	d_{31} [C/N]	d_{33} [C/N]	$\varepsilon_{33}^T/\varepsilon^0$	$\varepsilon_{11}^T/\varepsilon^0$
675×10^{-12}	-230×10^{-12}	500×10^{-12}	2200	2250

2.2 Operation principle of DSPLM

The linear motion of the newly developed linear motor is operated by the principle of inertia displacement, which can be explained by a saw tooth electrical potential as shown in Fig. 2 (a), (b). Figure 2 (a) shows the motion of a mobile element induced by the DSPA. When a mobile element locates at position l_a in Fig. 2 (a), the electric potential is not applied, represented as "a" position in Fig. 2 (b), which is called the initial state. During a gentle rise in the drive signal applied to the DSPA (a-b position in Fig. 2 (b)), the DSPA will slowly expand. Accordingly, the mobile element coupled with the drive shaft by friction will move to the upper direction, represented as position l_b in Fig. 2 (a). As the electric potential suddenly falls to the "c" position in Fig. 2 (b), which is the minimum electric potential, the DSPA moves to downwards. At this time, slip occurs between the shaft and the moving part because of the inertia force and the moving part does not substantially move and thus only the shaft returns to the initial position (l_a). Therefore, the mobile element changes position with the distance of l_b-l_a. Consequently, the mobile element will move repeatedly when the drive signal is applied for a desired number of times. If the slope of the saw tooth in the electrical potential is reversed, the direction of the mobile element would be reversed. It can be stated that the DSPLM proposed here realizes the principle of inertial displacement [7].

3 FEM analysis

The FEM code ATILA has been used in the simulation of the DSPA combined with shaft. The DSPA combined with shaft was drawn and meshed as shown in Fig. 3 (a), (b). It uses the dome-shaped piezoelectric ceramics of 9.86 mm in diameter and 4.6 mm in curvature of radius with 0.40 mm of thickness. The shaft made of carbon fiber reinforced plastic is used to provide a linear motion and length was varied from 15 mm to 30 mm. The piezoelectric, dielectric and elastic constants of PZT5AH, used in the FEM modeling, are shown in Table 1 [8].

Figure 4 shows the electrical impedance versus frequency, computed for a DSPA having different shaft length. It appears on these three graphs that two coupled modes exist; the first resonance frequency is around 87 kHz, the second resonance frequency is around 206 kHz under the free state of DSPA.

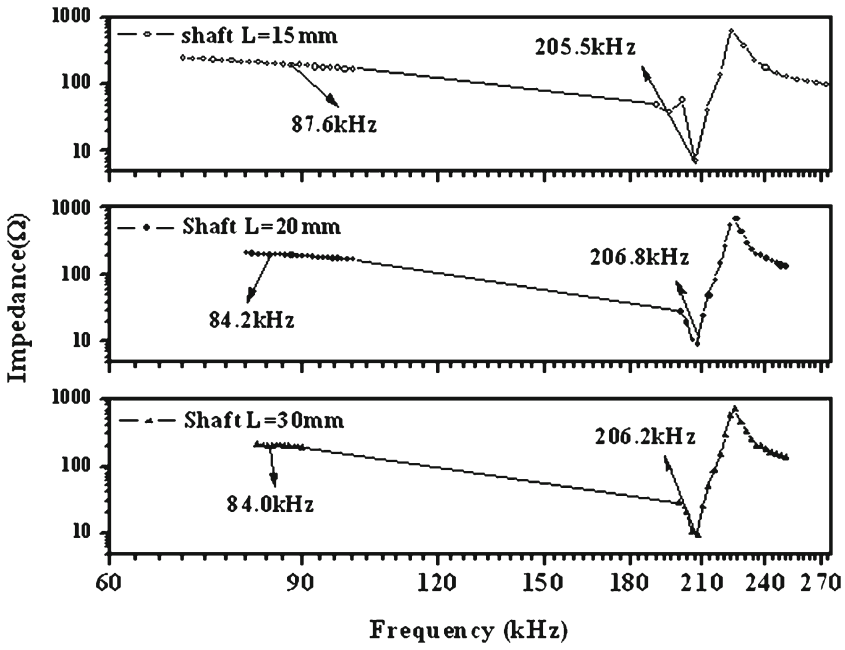

Fig. 4 Simulated impedance versus frequency curves for the DSPLM with the non-clamped bottom side

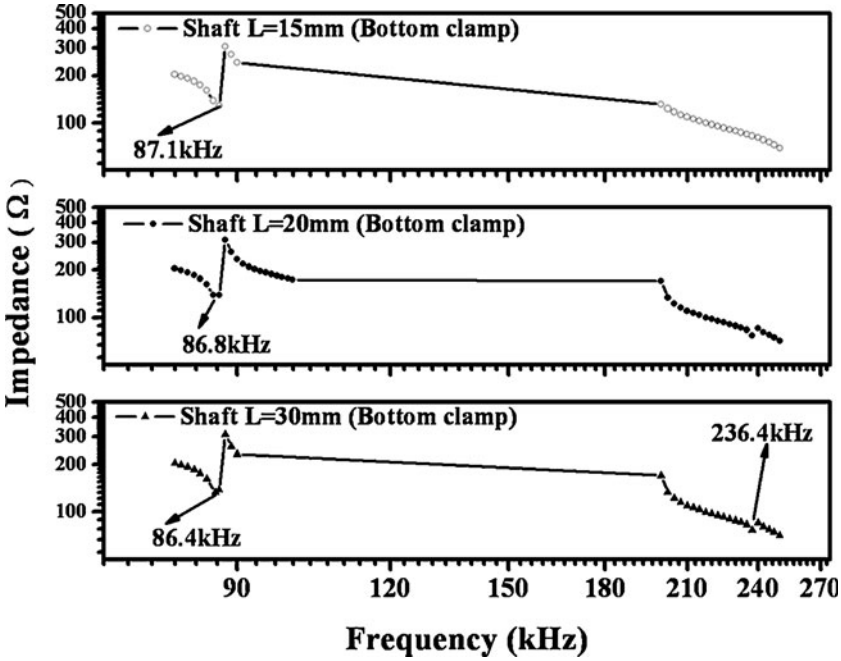

Fig. 5 Simulated impedance versus frequency curves for the DSPLM with the clamped bottom side

As shown in Fig. 4, 1st resonance frequencies decrease slightly with increased shaft length. In order to increase Z-axis vibration, the bottom side of DSPA was clamped by controlling the boundary condition of ATILA program, and a resonance frequency is computed again at the same shaft length. As shown in Fig. 5, the 1st resonance peak significantly appeared, resulting in the slight increase of the 1st resonance frequency compared to non-clamped state and the 2nd resonance peak nearly disappeared. It can be speculated that the clamping state may increase the Z-axis vibration mode of the DSPA with constraining the radial mode vibration.

The vibration displacement simulation of the DSPA was performed by ATILA FEM software to determine the maximum displacement for 30 mm shaft length at the 1st and 2nd resonance frequencies. The 1st and 2nd resonance frequencies correspond to λ and 3λ-mode of shaft, respectively. Figure 6 (a), (b) shows the axial vibration displacements of the non-clamped sample computed at the 1st and 2nd resonance frequencies by applying a electric field of $70V_{p\text{-}p}$ to DSPA. These results indicate that the maximum tip displacements of the Z-axis at the 1st and 2nd resonance frequencies are ±0.657 μm and ±3.576 μm, respectively. Note that the maximum tip displacement increases at the 2nd resonance frequency because of the lower impedance of radial vibration. On the other hand, in case of the bottom clamped DSPA, maximum tip displacement increases up to ±7.13 μm at the 1st resonance frequency

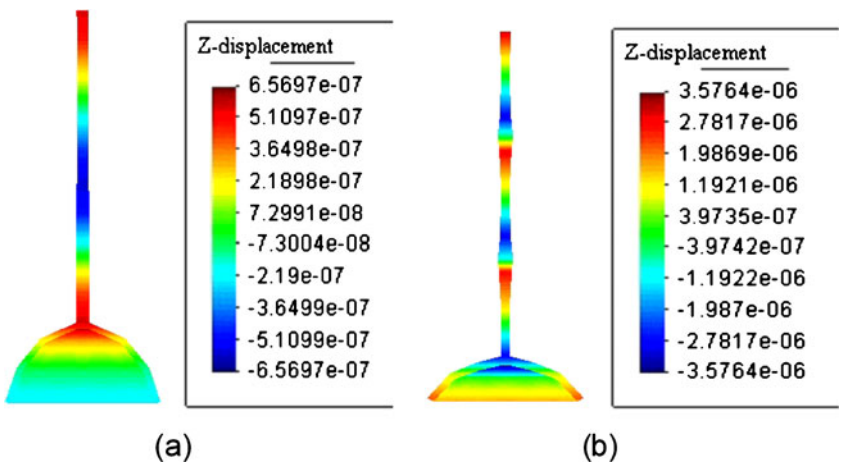

Fig. 6 ATILA 3-D simulation results for maximum axial displacement for (**a**) 1st and (**b**) 2nd resonance frequency with the non-clamped bottom side

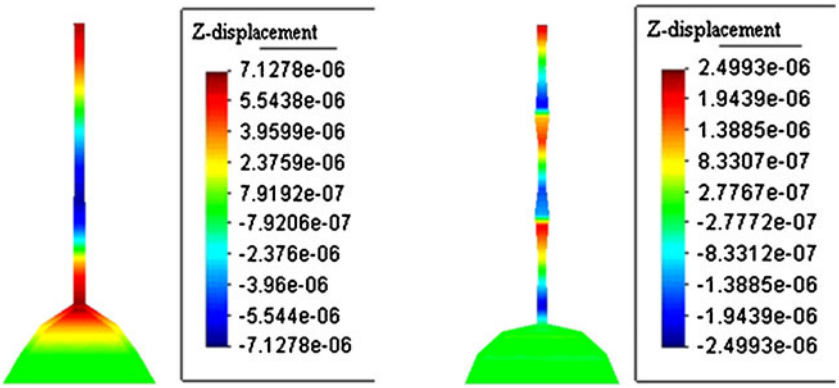

Fig. 7 ATILA 3-D simulation results for maximum axial displacement for (**a**) 1st and (**b**) 2nd resonance frequency with the clamped bottom side

and maximum tip displacement at the 2nd resonance frequency decreases to ±2.499 μm because of restricting the radial vibration mode due to the bottom constraining force as shown in Fig. 7. From these computed results, it can be predicted that clamping state obviously increases the Z-axis displacement of the DSPA at the 1st resonance frequency.

4 Experimental analysis of DSPA

4.1 Manufacturing process

To verify that the DSPA is applicable to ultrasonic linear motor, a $0.04Pb(Sb_{0.5}Nb_{0.5})O_3$-$0.46PbTiO_3$-$0.5PbZrO_3$ composition, which is generally used for a bimorph actuator, was used to fabricate DSPA. Preliminary study indicated that this composition is characterized by excellent dielectric/piezoelectric properties (d_{33}~550 pC/N, k_{33}^T~1950, k_p=0.7 at room temperature which values are different from PZT5A, used in the modeling) and high Curie temperature (T_c=320). The detailed fabrication process was shown in Fig. 8.

The PIM process has been described in detail. The binder usually based on a common thermoplastic such as wax of polyethylene. The binder system consists of three components. An example binder that is molten at 150°C consists of 60% paraffin wax, 35% polypropylene and 5% stearic acid. The binder content is approximately 40 vol.% of the mixture. The median particle size of piezoelectric powder is 0.85 μm with near spherical shape. The powder-binder mixture is pelletized and injection molded into dome shape. After injection molding, the binder is removed from component by a solvent and thermal debinding. After debinding, the specimen was sintered by placing an equimolar mixture of PbO and ZrO_2 inside a covered alumina crucible to minimize PbO loss. The sintered DSPA fabricated by PIM has diameter of 9.86 mm, curvature radius of 4.53 mm and thickness of 0.40 mm with shrinkage rate of 21%.

4.2 Impedance analysis and dynamic displacement measurement

Dome-shaped piezoelectric ceramic specimen were electroded with silver paste (Metech Inc. #3288) fired at 650°C for 30 min, and then poled in a stirred silicone oil bath at 150°C by applying a dc electric field of 2.5 kV/mm for 40 min. For constraining the radial mode vibration of bottom side, the ring-shaped ceramic was then bonded by epoxy.

In order to compare with simulation results, impedance curve over a frequency range from 10 to 300 kHz was measured by an impedance analyzer (HP 4194A) and the tip displacement at 1 resonance frequency was measured by applying an alternating square wave of $60V_{p\text{-}p}$ using the test equipments. The shaft of DSPA fixed at the top has length of 30 mm. Micro Laser Interferometer (Canon, DS-80) was used as a non-contact displacement sensor and driving voltage was applied by self-made circuit. The prototype sample was manufactured to measure the continuous linear motion under 10 g loads as shown in Fig. 9. The actuating part is composed of DSPA combined with clamping element, which is driven by self-made PWM circuit. As shown in Fig. 10, the mobile element also consists of three parts, which are the rigid metal for the inertia weight (10 g), such as alloy metal, a pair of L-shaped moving pieces made of phosphor bronze and plate spring fixed by bolt, which puts the pressure on the L-shaped plate spring in order to adjust the fictional force. Thus, mobile elements are compressed on the surface of the shaft by controlling the bolt passing through the one end of the plate spring. The dynamic linear motion of DSPLM was measured using a self-made driving circuit, which generates $60V_{p\text{-}p}$ at a 1 resonance frequency of 50 kHz and controlled by customer I.C. Pulse width modulation method is able to control the up and down moving direction because it can control the expansion and contraction velocity of piezoelectric element as it is

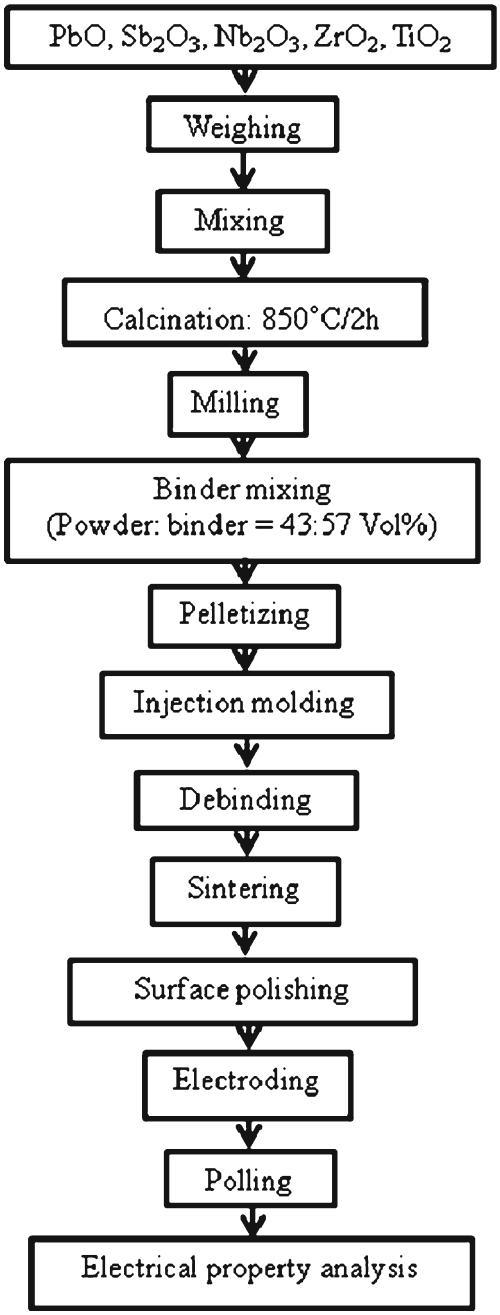

Fig. 8 Schematic representation of fabrication process

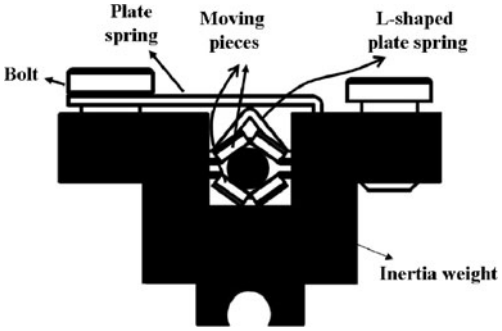

Fig. 10 Detailed schematic view of mobile element

possible for PWM method to reverse the phase of pulse width [9]. The continuous moving displacement properties of upper direction were measured at an applied 5 pulse with a Micro Laser Interferometer (Canon, DS-80A) having a resolution of 0.08 nm. During the measurement, the DSPLM was attached to a test fixture and the laser beam was focused on the inertia weight combined with shaft. All test devices were located on the optic table to isolate them from external vibration. The applied voltage and displacement signal were measured by voltage probe and recorded in the oscilloscope.

5 Results and discussion

In order to validate the results obtained by simulations, the bottom side clamped DSPA was manufactured by following FEM design. To compare the electric impedance of simulation with that of experimental data, the impedance vs. frequency curves are measured. Note that 1^{st} and 2^{nd} modes appear between 50 and 100 kHz under the clamped state as shown in Fig. 11. Moreover, the 1^{st} resonance frequency of the bottom-clamped DSPA decreases to 50 kHz. The decrease of 1^{st} resonance frequency is caused by increasing the total mass

Fig. 9 Schematic view and photograph of the manufactured prototype DSPLM

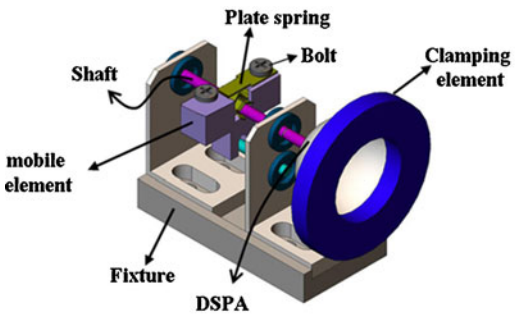

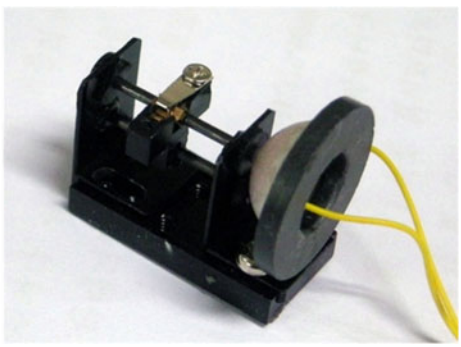

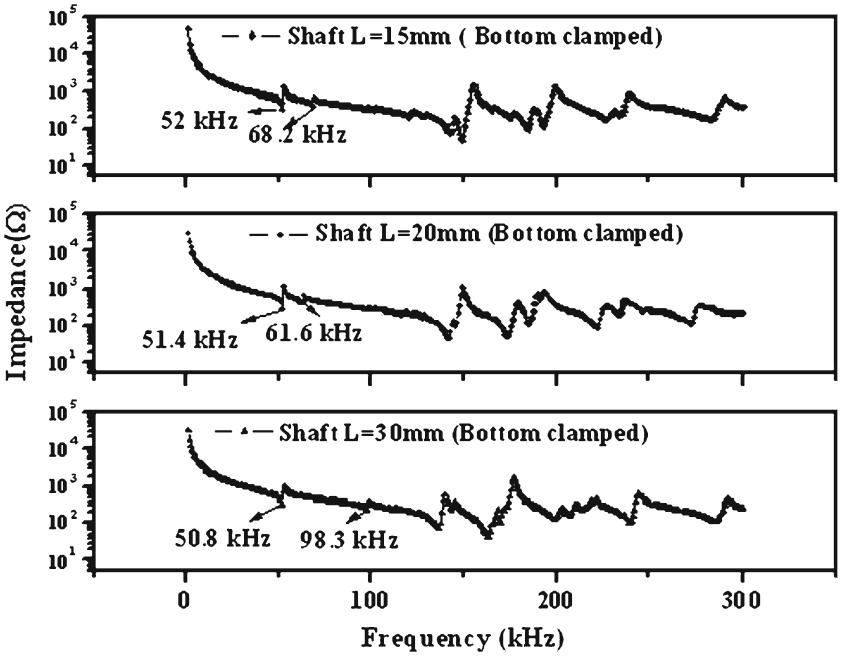

Fig. 11 Experimental data of impedance versus frequency curves for the DSPLM with the clamped bottom side

of DSPA due to bottom-clamped ceramic element. In general, the effect of mass on the resonance frequency can be described by following equation

$$f_r = \frac{1}{2\pi}\sqrt{\frac{s}{m}}$$

Where, f_r denotes the resonance frequency, S is the stiffness, m is the total mass. According to this equation, the resonance frequency decreases at the inverse square root of the total mass. The ceramic element combined with the bottom-side of DSPLM increased the total mass of DSPLM from 1.02 g to 2.0 g. Consequently, the resonance frequency decreased to 50 kHz. In case of simulation, only the bottom-side of DSPA was clamped. However, the clamping structure of experimentally manufactured sample was combined with bottom clamping ceramic element using the epoxy, which can make different resonance frequencies from simulation results. In spite of some discordance between resonance frequencies, it can be concluded that various vibration modes are caused by bottom-clamped ceramic

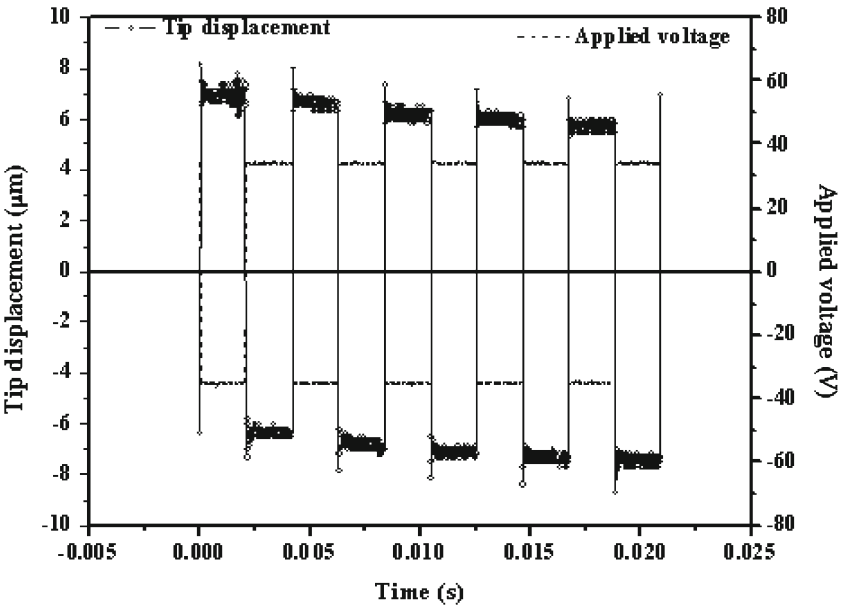

Fig. 12 The Z-axial tip vibration displacements and applied voltage for DSPLM

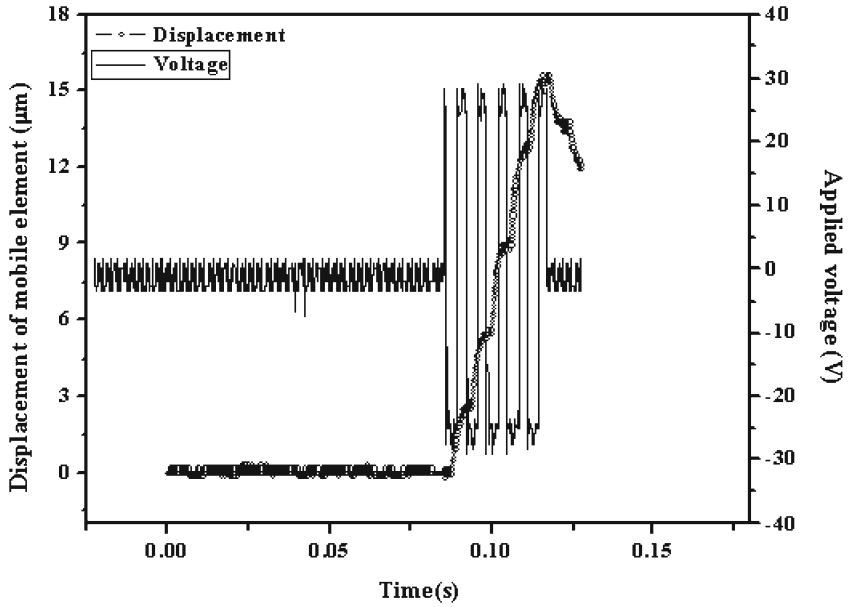

Fig. 13 The total displacement of DSPLM according to apply a voltage at 1 resonance frequency

element combined with DSPA and bonding material. Because of sampling speed limitation of displacement measuring instrument, the measurement of the displacement is limited to 1 resonance frequency (about 50 kHz). As shown in Fig. 12, the tip displacement property of DSPA combined with shaft and bottom clamping ceramic at 1 resonance frequency was ±7.48 μm under the electric field of $60V_{p\text{-}p}$

In spite of small size, the DSPA manufactured by PIM process has a large tip displacement, which is in accordance with the FEM results. This result indicates again that PIM process is very useful and simple method to make a large strain actuator.

To evaluate the continuous linear motion of DSPLM with inertia weight, the dynamic displacement characteristic of the prototype sample was performed. Figure 13 shows continuous moving displacement during five pulses applied to DSPLM, the total displacement of DSPLM was 15.6 μm. From these results, dividing 5 into the total displacement, we can get the displacement per pulse of 3.12 μm under 10 g load. Furthermore, the inertia and frictional behavior was observed from the results of the step-like displacement. The rapid increasing of displacement indicates that frictional force is larger than inertia force and the mobile element move together with shaft during a wide pulse width applied to DSPLM. On the other hand, during a narrow pulse width applied to DSPLM, the increase of displacement becomes almost zero. This denotes that inertia force is larger than frictional force and the mobile element does not fall down with shaft. As it can be seen, the displacement of the DSPLM combined with the proposed mobile element is smaller than the simulated one (about 50%). This behavior can be explained by load effect of inertia weight (10 g).

6 Conclusions

In this work, a new-typed high displacement ultrasonic actuator and an ultrasonic linear motor have been proposed. The former is composed of dome-shaped piezoelectric ceramic combined with shaft and bottom-clamped ceramic element. The latter consists of three parts, which were an actuating part, shaft, and mobile element. Design and analysis of high displacement ultrasonic actuator have been performed by using the ATILA FEM software. Performances of the experimentally fabricated actuator have been compared with that of simulation results.

Simulation results have shown that the bottom side clamping condition obviously exhibits displacement amplification about ten times higher than the non clamped condition at the 1st resonance frequency. Experimental comparison between maximum displacements substantially validated simulated results.

The prototype of a new type linear motor using a dome-shaped piezoelectric actuator has been also manufactured. To evaluate the continuous linear motion of DSPLM with inertia weight, the dynamic displacement characteristic of the prototype sample was performed. During five pulses applied to DSPLM, the total displacement of DSPLM was 15.6 μm. From these results, it could be concluded that the displacement per pulse was 3.12 μm under 10 g load. Therefore, the controllable accuracy of DSPLM is 3.12 μm.

The proposed linear motor, in conclusion, seems to be more suitable than the classical one in application where high displacement and accuracy are required and, furthermore, it is reduced in its total dimension and weight. The

possibility of further increase of resolution and decrease of total dimension, by decreasing the size of the dome-shaped piezoelectric ceramic, is currently under the study.

Acknowledgements This research was supported by the Program for the Training of Graduate Students in Regional Strategic Industries and Regional Innovation Center (RIC) Program which was conducted by the Ministry of Commerce, Industry and Energy of the Korean Government.

References

1. A. Furuta, K. Uchino, J. Am. Ceram. Soc. **76**, 1615 (1993)
2. H. Honmou, R. Ishikawa, S. Takahashi, Jap. J. App. Phys. **24** (Supplement 24-3), 187 (1985)
3. K. Uchino, Am. Ceram. Soc. Bull. **65**, 647 (1986)
4. K. Uchino, M. Yoshizaki, K. Kasai, H. Yamamura, N. Sakai, H. Asakura, Jap. J. App. Phys. **26**, 1046 (1987)
5. S. Ueha, Y. Tomikawa, M. Kurosawa, N. Nakamura, *Ultrasonic mortors: Theory and application* (Clarendon, Oxford, 1993), pp. 224–229
6. T. Hemsel, M. Mracek, J. Twiefel, P. Vasiljev, Ultrasonics **44**(1), 591 (2006)
7. K. Spanner, Piezoelectic Motors & Actuators (PI Presentations & Papers: ACTUATOR 2006 Conference in Bremen)
8. D.A. Berlincourt, D.R. Curran, H. Jaffe, in *Physical acoustics-principles and methods vol. 1-Part A*, ed. by W.P. Mason (Academic, New York, 1964), p. 169
9. US Patent 6815871 B2 (Drive mechanism and drive method employing circuit for generating saw-tooth waveform voltage.